

# A novel method for measuring carrier lifetime and capture cross-section by using the negative resistance $I$ – $V$ characteristics of a barrier-type thyristor

Li Hairong(李海蓉)<sup>†</sup> and Li Siyuan(李思渊)

(Institute of Microelectronics, Lanzhou University, Lanzhou 730000, China)

**Abstract:** A brand new and feasible method for measuring the carrier lifetime and capture cross-section of a barrier by using the negative resistance segment of the  $I$ – $V$  characteristics of a barrier-type thyristor (BTH) is put forward. The measuring principle and calculation method are given. The BTH samples are experimentally measured and the results are analyzed in detail.

**Key words:** carrier lifetime; capture cross-section; barrier-type thyristor

**DOI:** 10.1088/1674-4926/31/8/084005

**PACC:** 6855; 7340Q; 7340T

**EEACC:** 2550; 2560R

## 1. Features of the $I$ – $V$ characteristics of BTH

Although there are many kinds of methods for measuring the carrier lifetime and capture-cross section<sup>[1–4]</sup>, it is hard to satisfy the requirement that the method should be simple, convenient and nondestructive for on-line measurements of the processing line. In this paper a method for measuring carrier lifetime and capture cross-section by using the negative resistance  $I$ – $V$  characteristic segment when a barrier-type thyristor (BTH) transits from a blocking to a conducting state is presented. The experiment results indicate that the method is visual, accurate and reliable. Therefore, the BTH used and its  $I$ – $V$  characteristics are introduced here first. It is taken into account that the BTH made by the authors is a normally-off device during the structure design and fabrication. The device structure and its parameters are shown in Fig. 1.

The  $I$ – $V$  characteristics of BTH are given in Fig. 2. Figure 2(a) shows the forward characteristics of the conducting-state which is characterized by large current and very low conducting-state voltage drop. The forward blocking-state characteristic with small current flow is shown in Fig. 2(b). Since the gate is reverse biased, it exhibits triode-like characteristics as a static induction transistor (SIT). Figure 2(c) shows the negative resistance  $I$ – $V$  characteristics, which corresponding to the transition of the BTH from the forward blocking-state to conducting-state that are exactly the characteristics we used in measuring.

For the convenience of analysis, Figure 3 shows a diagrammatic sketch of one  $I$ – $V$  transition characteristic curve of the BTH which is shown in Fig. 2(c). The curve  $BF$  is the negative resistance snapback segment of the  $I$ – $V$  characteristics and represents the inevitable transition process before the BTH enters the conducting-state. It begins from point  $B$  and finishes at point  $F$ , which indicates that the BTH turns into the conducting-state completely. The nature and features of the turning point and curve  $BF$  have been studied in detail in another paper. In that paper, the authors studied simultaneously the causes and conditions that formed the negative resistance snapback segment of the  $I$ – $V$  characteristics of the BTH. Here it is necessary to enumerate the main points of view as follows:

(1) The curve  $BF$  represents the turn-on line of the BTH. The process before the point  $B$  is a preparatory stage. The device enters a critical and dynamic state when it reaches the point  $B$  and at this time all parameters change rapidly. The point  $B$  has the feature of duality, so it is neither a turn-on nor a turn-off point.

(2) Since the device is entering the conducting-state, the barrier should not exit on the current passage. Thus it indicates that the point  $B$  is the position where the barrier is flattened.

(3) The current is unipolar electron current before the point  $B$ ,  $j_A \approx j_n$ . From the point  $B$ , the BTH enters into a bipolar-state, and the electrons and holes are injected from the anode and cathode, respectively, which results in the formation of high density plasma. Thus, point  $B$  is also the transition point from a unipolar to a bipolar state.

(4) The point  $B$  depicts that the device is entering into a high-level injection state. All the high-level effects operate.

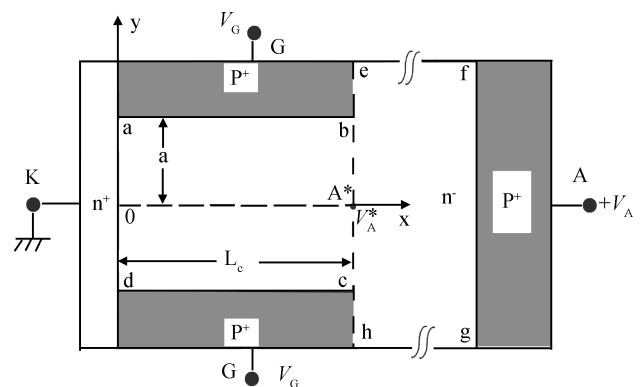


Fig. 1. Device structure of BTH. The device parameters are as follows: wafer thickness  $T = 300 \mu\text{m}$ ; width of lightly-doped  $n^-$  region  $W_n = 180 \mu\text{m}$ ; anode length  $L_A = 120 \mu\text{m}$ ; gate-to-gate half spacing  $a = 8 \mu\text{m}$ ; channel length  $L_c \approx L_G = 11 \mu\text{m}$ ; gate length  $L_G = 11 \mu\text{m}$ ; channel impurity concentration  $N_D^- = 5 \times 10^{13} \text{ cm}^{-3}$ ; gate impurity concentration  $N_A^+ = 5 \times 10^{18} \text{ cm}^{-3}$ ; cathode impurity concentration  $N_D^+ = 5 \times 10^{20} \text{ cm}^{-3}$ ; anode impurity concentration  $N_{AA}^+ = 2 \times 10^{18} \text{ cm}^{-3}$ .

<sup>†</sup> Corresponding author. Email: hrli@lzu.edu.cn

Received 23 February 2010, revised manuscript received 24 March 2010

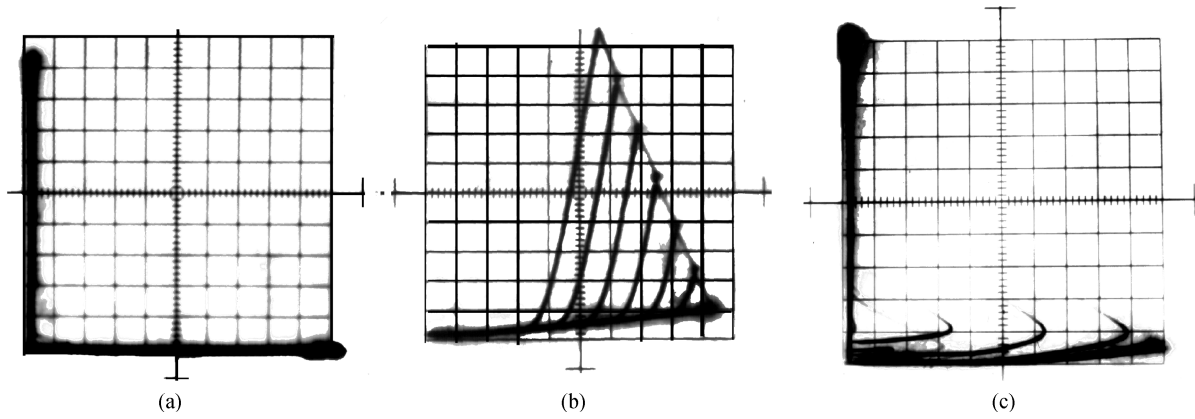


Fig. 2.  $I$ - $V$  characteristics of devices. (a) Forward conducting-state with large current (div:  $y$ : 1 A;  $x$ : 10 V). (b) Forward blocking-state with small current (div:  $y$ : 0.1 mA;  $x$ : 50 V). (c) Negative resistance characteristics of the transition from forward blocking to conducting state (div:  $y$ : 20 mA;  $x$ : 50 V).

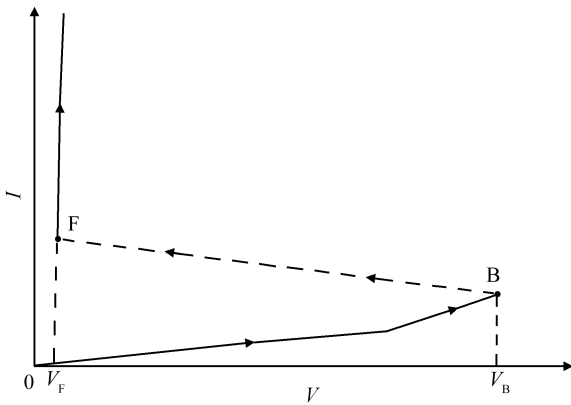


Fig. 3. Diagrammatic sketch of the BTH's transition characteristics.

Therefore, point  $B$  is the turning point from low-level to high-level injection as well.

(5) From the point  $B$  the  $I$ - $V$  characteristic starts the segment of negative resistance characteristics,  $\frac{dV}{dI} < 0$  ( $dV < 0, dI > 0$ ).

(6) From the point  $B$  the current changes from barrier-controlled current to double injection current that has an unequal lifetime<sup>[5]</sup>.

(7) The conductance modulation is the basic feature and the linchpin of transition process. It is ineluctable that the effective resistance of BTH itself varies from very high resistance in the blocking-state to extremely low resistance ( $\approx 0$ ) now.

## 2. Increase of the hole lifetime under high-level carrier injection

The channel barrier is similar to a 'sluice gate'. Once the 'sluice gate' opens, electrons and holes enter into the  $n^-$  base region including the channel and drifting region as majority and minority carriers from the cathode and anode, respectively, under high-level injection. In this case the double injection effect is established. The double injection effect is a kind of physical phenomenon generally existing in power devices. It is impossible to realize deep conductance modulation without the double injection effect, i.e., holes taking part in the current con-

duction. Hence it cannot realize the negative resistance transition and large current transfer. For the BTH, the key for establishing the double injection effect is that the injected minority carriers can pass through the drifting region and reach the cathode. This means that the transit time for holes from anode to cathode  $t_p$  should not at least be longer than its lifetime  $\tau_p$ , i.e.,

$$t_p = \frac{W_n^2}{\mu_p V_B} \leq \tau_p, \quad (1)$$

where  $\mu_p$  is the mobility of the hole, and  $V_B$  is the anode voltage corresponding to turning point  $B$ . It shows that with increasing anode voltage  $V_A$  the anode field  $E_A$  is enhanced continuously till it goes through the whole device, and the barrier can be flattened. Therefore holes can transit to the cathode and double injection is established. When the injection-level is high enough, a plasma filled with a high and equal density of holes and electrons is formed. Hence, under such conduction the filling situation of the recombination centers by carriers has changed significantly.

For the lightly doped n-Si base region, the conduction band electrons occupy the whole recombination center energy level  $E_t$  and tend to capture holes even under low-level injection state. For n-Si, only the deep acceptor state recombination centers are taken into account generally (for p-Si, the donator state recombination centers are considered instead). At present we only consider the acceptor-like type of the single recombination energy level and treat the variation of hole lifetime  $\tau_p$  approximatively by using single energy level recombination theory. There are two electrical states in this energy state: electronegative and neutral states. In this paper,  $n_0 = N_D^- = 5 \times 10^{13} \text{ cm}^{-3}$ , then  $p_0 = 4.5 \times 10^6 \text{ cm}^{-3}$ ,  $N_t = 1 \times 10^{11} \text{ cm}^{-3}$ .  $E_t$  is far under the Fermi energy level  $E_{Fn}$  and the shallow donor concentration of n-Si is higher than that of recombination centers,  $n_0/N_t = 5 \times 10^2$ . All recombination centers are fully filled with electrons, and hence exhibit negative electric centers under thermal equilibration state. Setting the capture cross-section of an empty neutral center for electrons in the conduction band as  $\sigma_n(\sigma_n^0)$ , the capture cross-section of negative electric centers for holes in the valence band is  $\sigma_p(\sigma_p^-)$ . In low-level injection, there is no possibility for recombination centers to capture electrons because they are already fully filled

with electrons, that is,  $\sigma_n^0$  is extremely small. Therefore the lifetime of electron  $\tau_n^0$  is very large and can even be considered to approach infinity. In contrast, because holes in the valence band are far less than negative electric centers,  $N_t/p_0 = 2.2 \times 10^4$ , all negative electric centers are ready tending to capture holes, i.e.,  $\sigma_p$  is quite large, which means that the lifetime of hole  $\tau_p$  is extremely small. Thus  $\sigma_n^0 \ll \sigma_p$ , or  $\tau_n^0 \gg \tau_p$ . Since the lifetime of holes injected from the anode is far less than its transit-time  $t_p$  from A to K, holes only exist in the near area of the anode without contribution to the current conduction and base region conductance modulation. The current is just space charge limited electron current<sup>[6]</sup> and is directly proportional to the square of the voltage. At this stage double injection cannot be formed yet.

When the anode voltage  $V_A$  increases to the flatten voltage  $V_{A,f}$ , the corresponding field  $E_{A,f}$  passes through the whole device up to the cathode. So the barrier is flattened under the action of  $E_{A,f}$ , resulting in the device quickly entering into high-level injection. Here there are enough hole filling centers (setting  $p = 5 \times 10^{18} \text{ cm}^{-3} \gg N_t = 1 \times 10^{11} \text{ cm}^{-3} \gg p_0 = 4.5 \times 10^6 \text{ cm}^{-3}$ ). In other words, because the holes in the valence band are abundant enough to absorb all electrons in centers, these centers reach a neutral state from the originally negative electric state. Therefore the  $\sigma_p$  becomes smaller and smaller, whereas  $\tau_{ph}$  is enlarged constantly.  $\tau_{ph} \gg \tau_p$ . All these are the consequences of the high-level effect. Therefore it becomes possible that (1) holes can transit through the whole base region up to the cathode; (2) double injection is formed; (3) e-h plasma is formed; (4) two kinds of carriers both contribute to current conduction and conductance modulation. When the concentrations of holes and electrons are very high ( $n \approx p \gg n_0 \approx N_D^-$ ), the main tendency in the base region is the recombination effect<sup>[7]</sup>. The speeds of recombination of holes and electrons can reach equilibration under the situation that all recombination centers are empty. Such a requirement is satisfied under high-level injection. So we have

$$\tau_{ph} = \tau_{nh}. \quad (2)$$

When we calculate electron lifetime under high level  $\tau_{nh}$ , the concentration of electron capturing centers is  $N_t$ , and hence  $\tau_{nh}$  can be expressed by

$$\tau_{nh} = \frac{1}{\bar{v}_n \sigma_n N_t}, \quad (3)$$

where  $\bar{v}_n$  is the average velocity of electrons.  $\tau_{ph}$  can be written as follows by using Eq. (2).

$$\tau_{ph} = \frac{1}{\bar{v}_n \sigma_n N_t}, \quad (4)$$

and the hole lifetime under low-level  $\tau_p$  is described as

$$\tau_p = \frac{1}{\bar{v}_p \sigma_p N_t}, \quad (5)$$

where  $\bar{v}_p$  is the average velocity of holes. If we consider approximately that the field  $E_{A,f}$  is large enough to make  $\bar{v}_p = \bar{v}_n \rightarrow v_{th}$ , the ratio of  $\tau_{ph}$  to  $\tau_p$  which corresponds to points  $F$  and  $B$ , respectively, is given by

$$\frac{\tau_{ph}}{\tau_p} = \frac{\sigma_p}{\sigma_n^0}. \quad (6)$$

In the situation of acceptor-like state recombination centers,  $\frac{\sigma_p}{\sigma_n^0}$  is about  $10^2-10^3$ . It is to say that along with the increase of the injected level, the numbers of holes are increasing. Therefore the current also becomes larger and larger, resulting in  $\tau_{ph}$  increasing quickly. So the transition of holes from A to K becomes easy. All injected holes from the anode have the ability to transit to the cathode and contribute to current conduction and conductance modulation.

### 3. A method for measuring the carrier lifetime and capture cross-section by using the negative resistance snapback segment

The negative resistance snapback segment represents the inevitable changing process before the BTH enters the conducting-state. It starts from the point  $B$  and terminates at the point  $F$ , which indicates that the BTH is completely in the conducting-state as shown in Fig. 3. As we mentioned above, the barrier is flattened when  $V_A$  increases to  $V_{A,f}$  which is represented by the point  $B$ . At this time, holes injected from the anode already have the ability to reach the cathode and can complete the electric current transfer and conductance modulation. The transit-time of holes from A to K can now be written as:

$$\tau_{pB} = \frac{W_n^2}{\mu_p V_{A,f}}. \quad (7)$$

This is almost the lifetime of holes under low-level injection, i.e.,

$$\tau_{pB} \approx \tau_p = \frac{1}{\bar{v}_p \sigma_p N_t} \approx \frac{W_n^2}{\mu_p V_{A,f}}. \quad (8)$$

Equation (8) yields:

$$V_{A,f} = \frac{W_n^2}{\mu_p \tau_p}, \quad (9)$$

where  $V_{A,f}$  is the voltage of the  $B$  point  $V_B$ .  $V_{A,f} = V_B$ . It is also the corresponding flatten voltage of barrier. When the device transits to the  $F$  point, that is,  $\tau_{ph} \gg \tau_p$ , the transit-time of the hole is expressed by:

$$\tau_{pF} = \frac{W_n^2}{\mu_p V_F} \approx \tau_{ph}. \quad (10)$$

So

$$V_F = \frac{W_n^2}{\mu_p \tau_{ph}}. \quad (11)$$

Comparing Eq. (9) with Eq. (11) and using Eq. (6), we get:

$$\frac{V_{A,f}}{V_F} = \frac{\tau_{ph}}{\tau_p} = \frac{\sigma_p}{\sigma_n^0} \gg 1. \quad (12)$$

$V_F$  is the forward voltage drop.  $V_F$  and  $V_{A,f}$  can be measured by the experimental method.  $\tau_p$  can also be measured during device fabrication processing. Thus  $\tau_{ph}$  is obtained by

$$\tau_{ph} = \frac{V_{A,f}}{V_F} \tau_p. \quad (13)$$

From  $S = \frac{\tau_{ph}}{\tau_p} - 1$ , we get:

Table 1. Main electric parameters of illustrative device samples.

| Parameter                      | Specification | 1                     | 2                     | 3                     | 4                     | 5                     | 6                     |
|--------------------------------|---------------|-----------------------|-----------------------|-----------------------|-----------------------|-----------------------|-----------------------|
| $V_B$ (V)                      | 1 mA          | 14                    | 48                    | 115                   | 248                   | 380                   | 516                   |
| $V_F$ (V)                      | 5 A           | 0.6                   | 0.7                   | 0.8                   | 1.1                   | 1.2                   | 1.2                   |
| $V_B/V_F$                      |               | 23                    | 69                    | 144                   | 225                   | 317                   | 430                   |
| $I_{AM}$ (A)                   | Heat-sink     | 22                    | 25                    | 23                    | 26                    | 25                    | 30                    |
| $V_{GK}$ (V)                   | 1 mA          | 8.8                   | 9.0                   | 7.8                   | 9.0                   | 8.8                   | 9.0                   |
| $t_{on}$ ( $\mu$ s)            | 60 V, 0.1 A   | 0.3                   | 0.2                   | 0.3                   | 0.4                   | 0.3                   | 0.3                   |
| $t_{off}$ ( $\mu$ s)           | 60 V, 0.1 A   | 1.2                   | 1.5                   | 2.1                   | 2.1                   | 4.0                   | 4.7                   |
| $\tau_{ph}$ ( $\mu$ s)         |               | 90                    | 274                   | 576                   | 900                   | 1268                  | 1720                  |
| $S$                            |               | 22                    | 68                    | 143                   | 224                   | 316                   | 429                   |
| $\tau_{no}$ ( $\mu$ s)         |               | 86                    | 270                   | 572                   | 896                   | 1264                  | 1716                  |
| $\sigma_n^0$ ( $cm^2$ )        |               | $1.2 \times 10^{-14}$ | $3.7 \times 10^{-15}$ | $1.7 \times 10^{-15}$ | $1.1 \times 10^{-15}$ | $7.9 \times 10^{-16}$ | $5.8 \times 10^{-16}$ |
| $\sigma_p$ ( $10^{-13} cm^2$ ) |               | 3                     | 3                     | 3                     | 3                     | 3                     | 3                     |
| $E$ ( $10^4 V/cm$ )            |               | 0.8                   | 3.0                   | 7.3                   | 15.7                  | 24                    | 32.5                  |
| $v/v_s$                        |               | 0.22                  | 0.50                  | 0.71                  | 0.84                  | 0.89                  | 0.92                  |

$$S = \frac{V_{A,f}}{V_F} - 1. \quad (14)$$

Then

$$S \equiv \frac{\tau_n^0}{\tau_p} \cong 0.827 \frac{\sigma_p}{\sigma_n^0}. \quad (15)$$

The low-level lifetime of electrons can be obtained as

$$\tau_n^0 = S\tau_p, \quad (16)$$

where  $S$  has no relationship with  $N_t$  and  $T$ . It is only determined by  $\frac{\sigma_p}{\sigma_n^0}$ .

Furthermore, according to

$$\sigma_n^0 = \frac{1}{v_{th}N_t\tau_n^0}, \quad (17)$$

we can get the low-level capture cross-section of electrons  $\sigma_n^0$ .

The low-level capture cross-section of holes,  $\sigma_p$ , is obtained by

$$\sigma_p = \frac{S\sigma_n^0}{0.827} \approx 1.21S\sigma_n^0. \quad (18)$$

Therefore, as long as the voltages that correspond to two ends of the negative resistance snapback segment (the points  $B$  and  $F$ ) are measured, we can get  $\tau_{ph}$  ( $= \tau_{nh}$ ),  $\tau_n^0$ ,  $\sigma_p$  and  $\sigma_n^0$ . This is a simple and convenient process measuring method and is sure to have certain value in the application of the device process. The method itself is of course approximate because we have used single energy level theory to treat carrier recombination and some approximate expressions were used in deducing the equations. However, what can be affirmed is that the two ends of the negative resistance snapback segment reflect the fact that their corresponding lifetime and capture cross-section of holes contain big differences. This kind of huge dissimilarity can be a kind of method to survey the parameters by all means.

#### 4. Experimental results and discussions

The experimental measuring results of the main electric parameters of BTH samples are listed in Table 1.

Figure 4 shows the channel field distribution corresponding to different gate voltages for the build up barrier  $V_{G,B}$  and

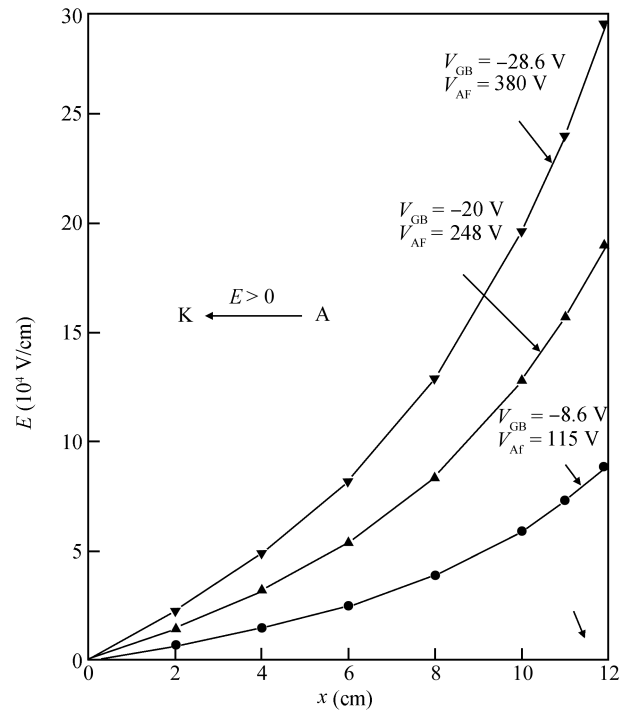


Fig. 4. Channel field distribution for variant  $V_{G,B}$  and  $V_{A,f}$ .

thus  $V_{A,f}$ . The field we used in Table 1 is the field at the channel end ( $x = 11 \mu m$ ) and the corresponding velocity of carrier  $v$  is calculated by using  $v(E) = v_s \frac{1}{1+E_s/E}$ , taking the correlation between velocity and field into account<sup>[5, 7]</sup>. Here  $v_s$  is the scattering terminal velocity which is about  $1 \times 10^7$  cm/s.  $E_s$  is the critical field that is calculated by using  $E_s \equiv \frac{V_s}{\mu_p}$ , where  $\mu_p$  is the low field mobility,  $\mu_p \cong 333$   $cm^2/(V \cdot s)$  and  $E_s \approx 3 \times 10^4$  V/cm. Studies indicate that  $\mu \propto E^{-1/2}$  and  $v \approx E^{1/2}$  under double injection conditions. When the field goes up to 8700 V/cm,  $v_s = v_{th}$ .

From Table 1 we can obtain the following conclusions:

(1) At high injection levels, the hole lifetime  $\tau_{ph}$  is almost equal to  $\tau_n^0$ . This indicates that the relationship between recombination centers which are fully filled by electrons and electrons in the conduction band is the same as that between the recombination centers which are fully filled by holes and holes

in the valence band.

(2) Lifetimes of holes under high and low injection levels are quite discrepant,  $\tau_{ph} \gg \tau_p$ .  $\frac{\tau_{ph}}{\tau_p}$  is about 22.5–430.

(3) Lifetimes of electrons at different injection levels show almost no variation, i.e.,  $\tau_{n,h} \approx \tau_n^0 \approx \tau_{ph}$ . This reflects the fact that the relationship between recombination centers and electrons in the conduction band is not impacted by injection level.

(4) The capture cross-section  $\sigma_n^0$  in Table 1 decreases from  $1.2 \times 10^{-14}$  to  $5.8 \times 10^{-16}$  cm<sup>2</sup> when the field increases from  $8 \times 10^3$  to  $3.25 \times 10^5$  V/cm because of the correlation between mobility and fields. Correspondingly, the lifetime of electrons  $\tau_n^0$  also goes up from 86 to 1716  $\mu$ s. Since  $\tau_{ph} \approx \tau_n^0$ , the lifetime of holes at high injection levels increases accordingly, becoming about 430 times the lifetime at low-level injection.

It should be pointed out that the capture cross-section of holes at low injection level  $\sigma_p$  ( $\sigma_p^-$ ) has been kept at a rather large value all along:  $\sigma_p = 3 \times 10^{-13}$  cm<sup>2</sup> ( $\sigma_p \gg \sigma_n^0$ ). It has not been affected by the enhancement of field or velocity change, because  $\sigma_p$  reflects what happens between recombination centers and holes in the valence band. However, there are no big changes for these two aspects at low injection level, i.e., (1) for lightly doped n<sup>-</sup> base,  $n_0 \approx N_D^- = 5 \times 10^{13}$  cm<sup>-3</sup>, few holes are in the valence band,  $p_0 \approx 4.5 \times 10^6$  cm<sup>-3</sup>. Also, its increase at a low-level is not great,  $p \ll n_0$ ,  $p \ll N_t$ . (2) Recombination centers are of acceptor-like type which are fully filled by electrons ( $N_t = 1 \times 10^{11}$  cm<sup>-3</sup>,  $N_t \ll n_0$ ) at a low-level and are all negative state. So they have a very strong capability to capture valence band holes. Therefore  $\sigma_p$  has been kept at a rather large value all along.

## 5. Conclusion

The characteristic of negative resistance is a special feature of transition, and the base conductance modulation is one of the

important reasons for this. The authors point out that the conditions and physical mechanisms of conductance modulation are as follows. (1) Double injection of carriers or plasma injection. (2) High enough injection level,  $n \approx p \gg n_0 \approx N_D$ . (3) Longer injected hole lifetime than the transit-time from A to K, which results in holes being able to transit the whole base region instead of being captured by recombination centers. (4) Change of the filling situation and making centers vary from the negative state to the neutral state. (5) Field enhancement to speed up the drifting velocity of carriers.

The authors put forward a brand new method for measuring the lifetime and capture cross-section of the carrier by using the negative resistance transition segment for the first time. The measuring principle and calculation method are also given. The BTH samples have been measured and the data results have been analyzed in this paper.

## References

- [1] Look D C, Fang Z Q, Sizelove J R. Accurate measurement of capture cross sections in deep level transient spectroscopy: application to EL2 in GaAs. *Journal of Electronic Materials*, 1995, 24(9): 1461
- [2] Macdonald D H, Geerligs L J, Azzizi A. Iron detection in crystalline silicon by carrier lifetime measurements for arbitrary injection and doping. *J Appl Phys*, 2004, 95(2): 1021
- [3] Schroder D K. *Semiconductor material and device characterization*. Hoboken, New Jersey, US: John Wiley & Sons Inc, 2006
- [4] Liu Xinfu, Du Zhanpin, Li Weimin. *Fundamentals and applications of semiconductor measurement technology*. Beijing: Metallurgical Industry Press, 2007 (in Chinese)
- [5] Wagener J L, Milnes A G. Double injection experiment in semi-insulating silicon diode. *Solid-State Electron*, 1965, 8: 495
- [6] Li Siyuan. *Action theory of the static induction devices*. Lanzhou: Lanzhou University Press, 1996 (in Chinese)
- [7] Lampert M A. Double injection in insulators. *Phys Rev*, 1962, 125(1): 126